ORIGINAL ARTICLES

School of Pharmacy[1], Nanchang University; Science and Education Department[2], Jiangxi Cancer Hospital, Nanchang, China

Improved gastrointestinal stability of solid lipid nanoparticles using comb-shaped amphiphilic inulin derivatives

Taoxing Peng[#,1], Feng Guo[#,1], Desheng Liang[#,1], Yuan Gao[2], Xiuying Zhang[1], Suping Qiu[1], Jian Liu[1], Haijun Zhong[1,*]

Received July 26, 2018, accepted November 11, 2018

**Corresponding author: Haijun Zhong, School of Pharmacy, Nanchang University, No. 461, Bayi Road, Donghu District, Nanchang 330006, Jiangxi Province, China
zhonghj@ncu.edu.cn
[#]These authors contributed equally to this work*

Pharmazie 74: 47–53 (2019) *doi: 10.1691/ph.2019.8140*

In order to reduce enzymatic degradation and thereby enhance the stability of solid lipid nanoparticles (SLNs) in the gastrointestinal tract, comb-shaped amphiphilic macromolecular material (CAM) of dodecyl inulin (Inu12) and octadecyl inulin (Inu18) were designed as the emulsifier and stabilizer to modify SLNs (Inu12/Inu18-SLNs). Inu12-SLNs and Inu18-SLNs had similar particle size as the control SLNs (P188-SLNs and Tween-SLNs) prepared with the straight chain surfactants, poloxamer 188 and tween-80 as the emulsifier, which ranged from 220 nm to 270 nm. The zeta potentials of all the SLNs formulations were slightly negative. Cyclosporine A (CsA)-loaded Inu12-SLNs and Inu18-SLNs showed a much lower drug release than CsA-loaded Tween-SLNs at pH 6.8 PBS containing 0.1% sodium dodecylsulfate and all the three SLNs exhibited biphasic release profiles. The results of cytotoxicity test showed that the toxic effects of Inu12-SLNs and Inu18-SLNs on cell viability had no significant difference in comparison to P188-SLNs and Tween-SLNs. Both CAM-modified SLNs (Inu12/Inu18-SLNs) showed a significant reduced lipolysis *in vitro*. As compared to P188-SLNs and Tween-SLNs, the total lipolysis of Inu18-SLNs during 4 h was decreased by 31.51 % and 45.67 % and that of Inu12-SLNs was decreased by 24.13 % and 38.29 %, respectively. Besides, the cumulative drug precipitations for CsA-loaded Inu12-SLNs and Inu18-SLNs during 4 h lipolysis were dramatically declined, which were 64% and 42% of that for Tween-SLNs, respectively. Therefore, it can be concluded that both alkylated inulin-derived CAM-modified SLNs, especially the Inu18-SLNs had the improved gastrointestinal stability to resist the lipid degradation by lipase enzyme.

1. Introduction

Solid lipid nanoparticles (SLNs) are a nano-sized drug delivery system using physiologically compatible lipids or waxes of high melting point as matrix materials (Thukral et al. 2014; Ban et al. 2017). SLNs have been widely used for oral delivery of various drugs, such as protein and peptides, poorly water-soluble small molecule drugs, and so on (Wang et al. 2018; De Jesus et al. 2015; Christophersen et al. 2014). Oral administration of SLNs is believed to be able to enhance the drug bioavailability, especially for the poorly water-soluble drugs by modulating their physico-chemical properties, protecting them against the harsh environment of gastrointestinal tract (GIT) and controlling the release kinetics (Małgorzata and Michał 2016; Talele et al. 2018; Shidhaye et al. 2008).

However, despite these advantages, the SLNs stability in GIT after oral administration has weakened the practical application of SLNs (Jannin et al. 2014). The material used for SLNs is usually glycerides, which are readily digested and degraded by lipase enzyme in the digestive tract after oral administration (Jannin et al. 2014; Feeney et al. 2014). After oral administration, SLNs may be digested and degraded easily by lipase and colipase in the digestive tract. This may result in the exposure of APIs incorporated in the SLNs (Warren et al. 2010). If the APIs incorporated belongs to poorly water-soluble small molecule drug, its precipitation would happen and then affect the absorption. If the incorporated APIs are instable or belong to peptide, protein or nucleid acids, they will suffer from the severe degradation and biological inactivation (Warren et al. 2013). Thus, it is imperative to conquer the obstacle of GIT instability of SLNs in oral administration.

In this work, comb-shaped amphiphilic macromolecular material (CAM), alkylated inulin derivative (Fig. 1), was fabricated as the emulsifier and stabilizer to modify SLNs for the first time. CAM consists of a homopolymer or copolymer backbone to which hydrophobic and hydrophilic pendant groups can be grafted resulting in a comb-like architecture. CAM has recently emerged as an alternative promising approach to amphiphilic block copolymers to prepare micelle and emulsion (Hoskins et al. 2012; Exerowa and Platikanov 2009; Tadros 2009). CAM possesses reduced critical aggregation concentration values compared with traditional straight-chain surfactant indicating increased micelle stability with decreased disruption (Exerowa and Platikanov 2009). Just as the emulsion with CAM as the emulsifier (Tadros 2009), using CAM with a hydrophilic backbone and hydrophobic branches as the emulsifier to prepare and modify SLNs, the hydrophilic chain of CAM on the surface of SLNs will assemble tooth-like loops and look like the petals of sunflower (Fig. 2). We hypothesized that the hydrophilic tooth-like loops of the CAM on the surface of SLNs

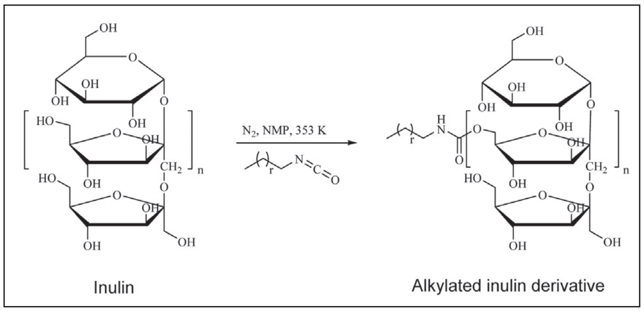

Fig. 1: Synthesis of inulin derivatives

might produce the steric hindrance effect and thereby enhance the GIT stability to resist the degradation of lipase enzyme.

Inulin is a natural, biocompatible and biodegradable polysaccharide, which typically consists of linear chains of b-(2-1) fructose units and a glucose unit attached at the reducing end (Imran et al. 2012). It is water soluble and the hydroxyl groups on its backbone are good for hydrophobic modification (Imran et al. 2012; Morros et al. 2010; Zhang et al. 2015). Here, we aimed to synthesize comb-shaped amphiphilic inulin derivatives with hydrophobic alkyl branched-chains to decorate SLNs. It was supposed that the lipid matrix of SLNs may be shielded from the degradation of lipase enzyme due to the steric hindrance effect of the hydrophilic tooth-like loops on the surface of SLNs formed by inulin derivatives.

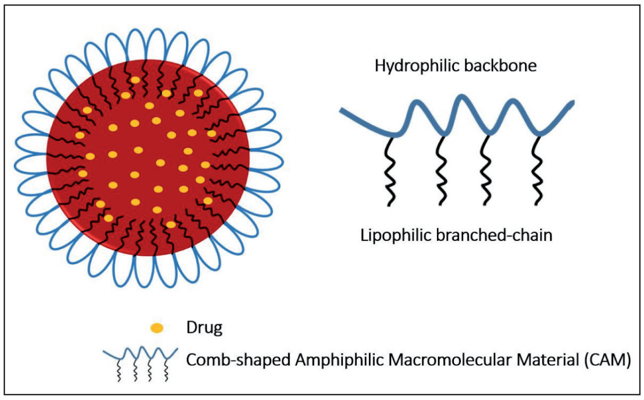

Fig. 2: Schematic diagram of comb-shaped amphiphilic inulin derivatives and SLNs.

To investigate the influence of alkyl chain length on the GIT stability of modified SLNs, octyl inulin (Inu8), dodecyl inulin (Inu12) and octadecyl inulin (Inu18) were synthesized by transesterification reaction in this study (Stevens et al. 2001). Then, three comb-shaped amphiphilic inulin derivatives were used as the emulsifier to prepare and modify SLNs. After the physio-chemical properties of modified SLNs were characterized, *in vitro* lipolysis behavior of SLNs in GIT simulated model was investigated. Finally, the cytotoxicity test of modified SLNs was conducted using human colon carcinoma cells lines to evaluate the safety preliminarily.

2. Investigations, results and discussion

2.1. *Synthesis of inulin derivatives*

FT-IR spectra of inulin and its alkyl derivatives are shown in Fig. 3. The inulin derivatives had much stronger infrared absorption at near 2850-2930 cm^{-1}, which corresponded to C-H stretching vibration of methyl and methylene group of alkyl chain. Meanwhile, the characteristic peaks of amide band I, II and III of inulin derivatives appeared at 1670-1710, 1540-1550 and 1200-1470 cm^{-1}, respectively. Figure 4 depicts ^{1}H NMR spectra of inulin and its alkyl derivatives. The spectra of inulin derivatives displayed two new peaks at d 0.85-1.25 ppm, which were attributed to the protons of CH_2 and CH_3 of alkyl chains, indicating the alkyl chains was successfully conjugated to the inulin backbone. The elemental analysis results for inulin and Inu8, Inu12 and Inu18 are shown in Table 1. The substitution degrees of Inu8, Inu12 and Inu18 were calculated to be 24.08 %, 34.49 % and 31.09 %, respectively.

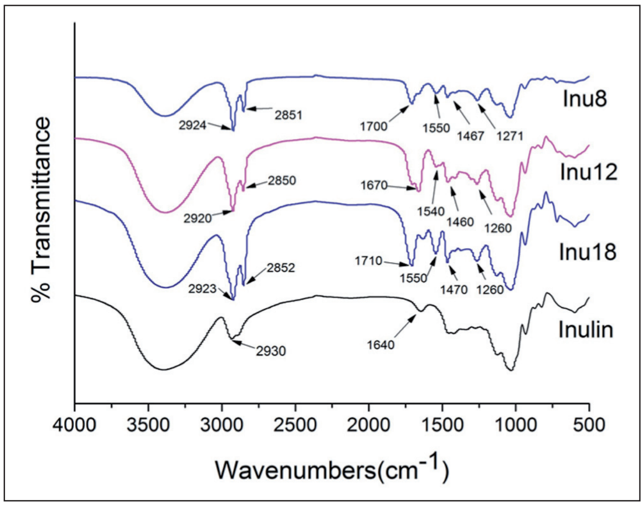

Fig. 3: FT-IR spectra of inulin and synthesized alkyl inulin derivatives.

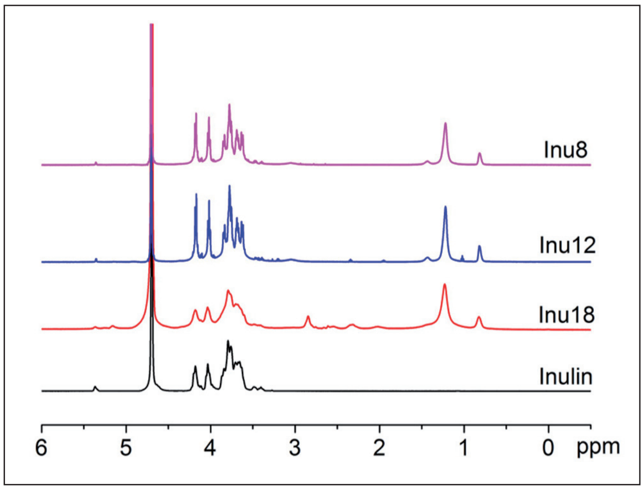

Fig. 4: ^{1}H NMR spectra of inulin and synthesized alkyl inulin derivatives.

Table 1: Chemical compositions and DS of inulin and its derivatives (means ± SD, n = 3)

Samples	C (%)	H (%)	N(%)	O (%)	DS(%)
Inulin	41.42±0.16	5.51±0.02	<0.3	52.11±0.29	—
Inu8	51.75±0.22	7.12±0.05	1.78±0.07	36.78±0.32	24.08
Inu12	54.18±0.24	7.64±0.10	2.08±0.05	33.40±0.37	34.49
Inu18	49.58±0.18	6.84±0.08	1.51±0.04	41.22±0.41	31.09

2.2. *Characteristics of SLNs*

To exclude the influence of particle size in *in vitro* lipolysis experiments, a systematic optimization of preparation process were carried out to obtain various SLNs with similar particle size. Inu8-SLNs underwent a visible precipitation soon after preparation. The possible reason for this was that the hydrophobic alkyl chains length of Inu8 was shorter than those of Inu12 and Inu18. Therefore, Inu8 could not effectively be embedded in the lipid matrix and had limited ability to improve the stability of the colloidal system. Besides, the gelation phenomenon occurred after Cyclosporine (CsA)-loaded P188-SLNs were prepared. Thus, Inu8-SLNs and CsA-loaded P188-SLN were not further characterized in the following work.

As shown in Table 2, the mean diameters of seven SLNs formulations ranged from 220 nm to 270 nm. Inu12-SLNs exhibited mean diameters of approximately 265 nm, which was slightly larger than Inu18-SLNs (less than 250 nm). The polydispersity indexes (PDI) of the modified SLNs were less than 0.3, indicating the uniform size distribution (Fig. 5). The zeta potentials of the modified SLNs were slightly negative. The encapsulation efficiencies of CsA-loaded Tween-SLNs, Inu12-SLNs and Inu18-SLNs were above 70% and the CsA loading contents were up to 6.5%. Fig. 6 shows the typical TEM images of SLNs. All the prepared SLNs were in spherical shape.

2.3. *Drug release in vitro*

As CsA is a poorly water-soluble drug, sodium dodecylsulfate (SDS) as a surfactant was added into the release medium to solubi-

Table 2: Particle size, zeta potential, encapsulation efficiency (EE) and drug loading (DL) of SLNs (means±SD, n=3)

SLNs	Particle Size(nm)	PDI	Zeta Potential (mV)	EE (%)	DL (%)
P188-SLNs	247.8±4.7	0.319±0.024	-11.8±0.7	-	-
Tween-SLNs	232.7±5.3	0.281±0.074	-10.1±1.7	-	-
Inu12-SLNs	269.1±15.4	0.211±0.046	-8.9±1.4	-	-
Inu18-SLNs	224.1±22.1	0.158±0.731	-5.8±1.6	-	-
CsA-loaded Tween-SLNs	245.2±6.3	0.278±0.112	-10.7±1.6	79.07±0.87	7.33±0.07
CsA-loaded Inu12-SLNs	263.4±12.6	0.217±0.043	-7.8±1.5	74.62±0.45	6.94±0.09
CsA-loaded Inu18-SLNs	245.1±7.5	0.237±0.034	-6.5±1.3	72.95±0.72	6.80±0.11

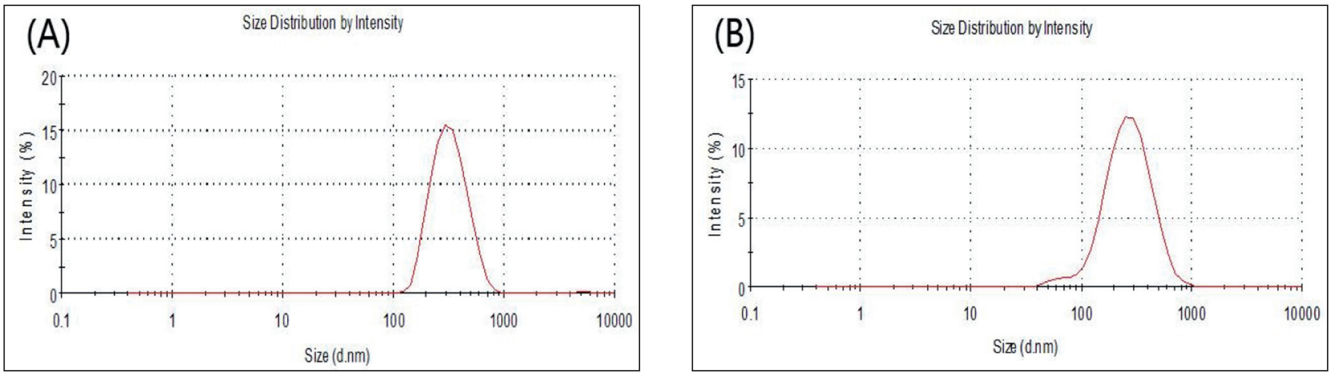

Fig. 5: Typical droplet size distribution diagram of SLNs. (A) CsA-loaded Inu12-SLNs, (B) CsA-loaded Inu18-SLNs.

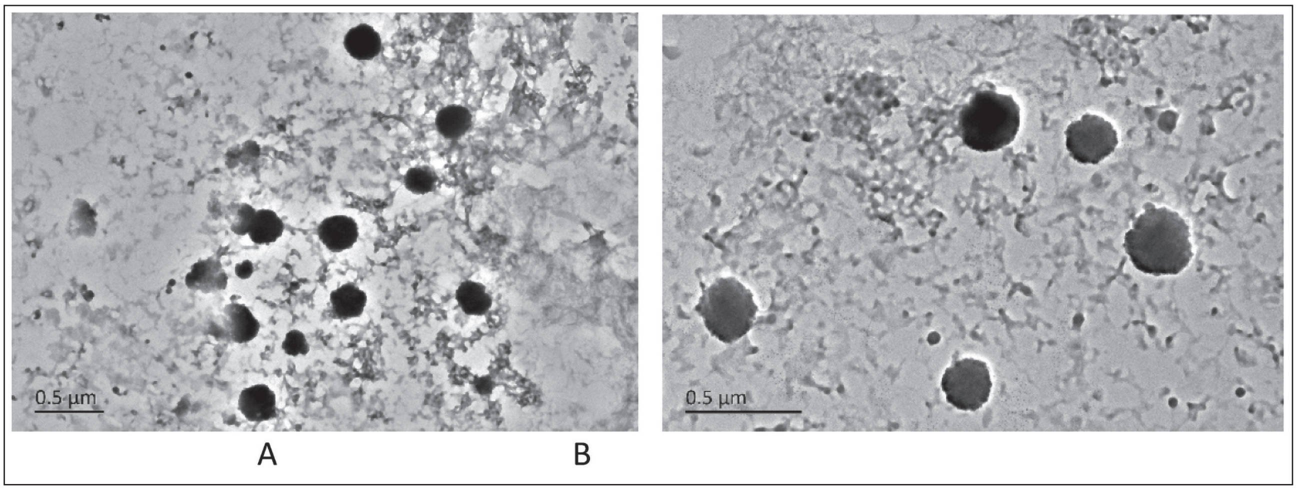

Fig. 6: Typical transmission electron microscopic images of SLNs. (A) Inu18-SLNs, (B) CsA-loaded Inu18-SLNs.

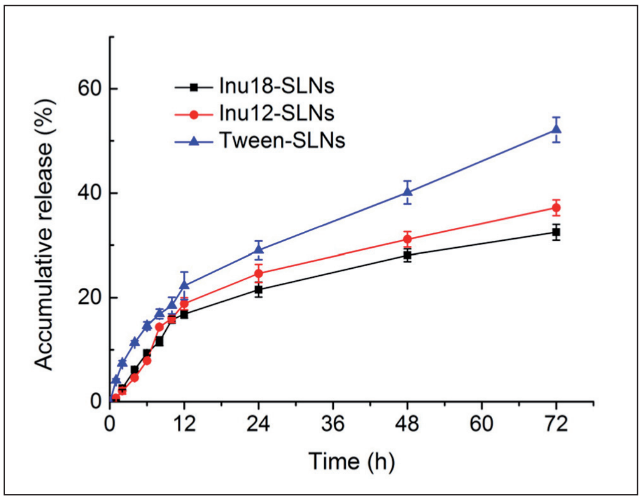

Fig. 7: *In vitro* release profiles of CsA-loaded SLNs at pH 6.8 PBS containing 0.1% (w/v) SDS (n=3).

lize the drug and ensure the sink condition. The solubilities of CsA at pH 6.8 phosphate buffer solution (PBS) containing different SDS concentration were determined before the experiment of drug release *in vitro* was conducted. The results showed that the solubilities of CsA at pH 6.8 PBS containing 0.05%, 0.1% and 0.2% (w/v) SDS were 78.87, 328.30 and 689.15 μg/mL, respectively. The drug concentrations at the release medium were calculated to be less than 19.20 μg/mL if the drug loaded in the three SLNs was completely released, which revealed that the sink condition could be maintained by adding 0.1% (w/v) SDS into the medium.

As depicted in Fig. 7, all the SLNs showed a slow drug release. The release of CsA at the initial 2 h was less than 10%. All the tested formulations exhibited biphasic release profiles with a fast drug release at the initial 12 h followed by a slow release. Tween-SLNs showed a faster CsA release than Inu12-SLNs and Inu18-SLNs did ($p<0.05$). The accumulative CsA release from Tween-SLNs during 72 h were 52.15%, while those for In12-SLNs and Inu18-SLNs were 37.18% and 32.49%, respectively. There was no significant difference between Inu12-SLNs and Inu18-SLNs.

2.4. Gastrointestinal tract stability study

As shown in Fig. 8, the cumulative amount of FFAs titrated of Inu18-SLNs, Inu12-SLNs, P188-SLNs and Tween-SLNs during 4 h lipolysis were 70.4, 89.5, 152.3 and 189.1 µmol, respectively. Inu18-SLNs and Inu12-SLNs had slower lipolysis rate as compared to P188-SLNs and Tween-SLNs. The amounts of FFAs titrated of Inu12-SLNs and Inu18-SLNs at each tested time point were lower than those of P188-SLNs and Tween-SLNs, which indicated the significantly decreased lipolysis rate for Inu12-SLNs and Inu18-SLNs. The total lipolysis extent during 4 h for Inu18-SLNs was decreased by 31.51% and 45.67%, respectively as compared with P188-SLNs and Tween-SLNs. Besides, Inu18-SLNs showed a slower lipolysis rate than Inu12-SLNs did. The total lipolysis extent of Inu18-SLNs was decreased by 7.37% as compared to Inu12-SLNs.

Due to the SLNs lipolysis, the loaded drug may suffer from the premature drug release and expose in GIT. This may lead to the drug precipitation in GIT if the drug incorporated in SLNs is water-insoluble. Therefore, drug precipitation during SLNs lipolysis *in vitro* was determined by using CsA as a representative drug. As shown in Fig. 9. CsA-loaded Inu18-SLNs and Inu12-SLNs had slower drug precipitation rate as compared to Tween-SLNs. The CsA precipitation percentages for Inu18-SLNs and Inu12-SLNs at each time point during 4 h were lower than that for Tween-SLNs. After 4 h of lipolysis, the percentages of cumulative drug precipitation of Inu18-SLNs and Inu12-SLNs were about 0.42 and 0.64 times that of Tween-SLNs, respectively. Obviously, Inu18-SLNs had the lowest drug precipitation during the lipid degradation. The results illustrated that the both inulin-derived CAM-modified SLNs (Inu18/Inu12-SLNs) could reduce the drug precipitation behavior of poorly water-soluble drug, and further confirmed that Inu18-SLNs and Inu12-SLNs produced strong resistance against the catalytic degradation by lipase enzyme and thereby had better gastrointestinal stability, especially Inu18-SLNs with long chain alkylated inulin as the emulsifier.

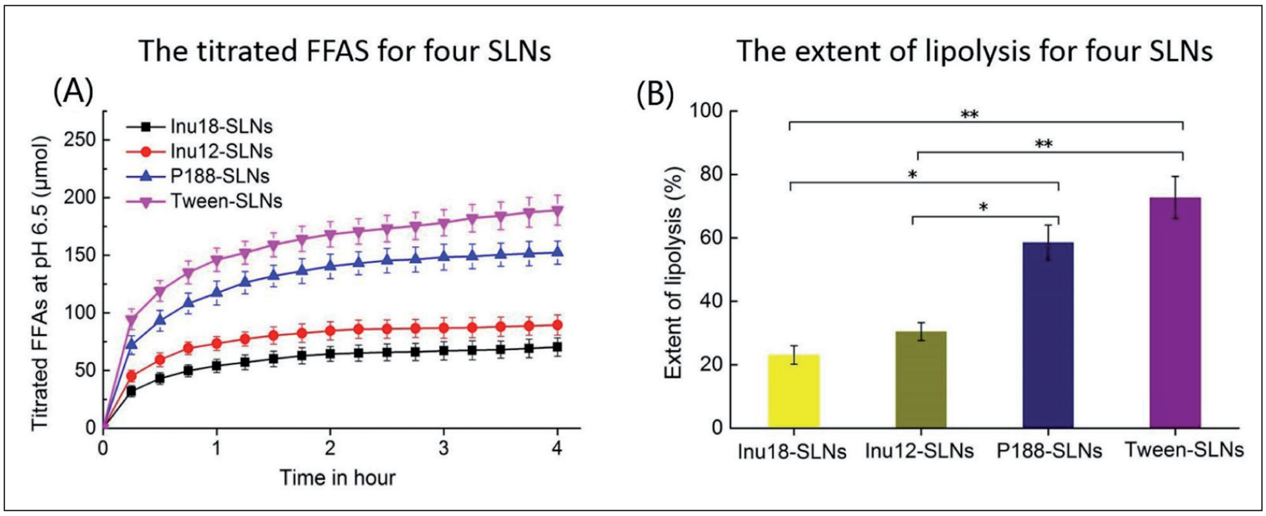

Fig. 8: Titrated FFAs (A) and the total lipolysis extent (B) of Inu18-SLNs, Inu12-SLNs, P188-SLNs and Tween-SLNs at pH 6.5 during 4 h of lipolysis. * represent $0.01<p<0.05$. ** represent $0.001<p<0.01$.

The reason for the better gastrointestinal stability of Inu18-SLNs and Inu12-SLNs may be that hydrophilic backbone of Inu18 and Inu12, a kind of CAM, could form dense sunflower-petal like loops on particle surface of SLNs, which might serve as a natural surface barrier (Fig. 2). The spatial or steric hindrance effect of the surface barrier could avoid the interaction between SLNs and lipase enzyme, thereby reducing lipid degradation and preventing the drug from exposure and precipitation in the digestive fluid.

As is known, hydrophilic polymers with straight chain (for example, PEG) modified on the surface of long-circulating or stealth microparticles may provide steric hindrance effect against the opsonins of the blood due to its hydrophilicity and flexibility (Torchilin 1998). Similarly, CAM with a hydrophilic backbone and hydrophobic branches modified on the surface of SLNs might also produce steric hindrance effect against lipase enzyme during the lipolysis. Moreover, the steric hindrance effect of CAM-modified SLNs might be stronger than that of straight chain polymer modified SLNs.

As depicted in Fig. 10, the flexible hydrophilic chains of adjacent molecules of straight chain polymer on the surface of SLNs might move apart toward different or even opposite directions at a certain moment due to molecular conformation transition, resulting in the interstices or spaces which might present the chance for lipase enzyme to contact the lipid matrix of SLNs and catalyze its degradation. However, it was not the case for CAM-modified SLNs. The dense sunflower-petal like loops on particle surface might protect lipids materials from lipase enzyme constantly. Therefore, the lipolysis of SLNs modified with alkylated inulin derivatives were slower than that of P188-SLNs or Tween-SLNs, which were modified with polyoxyethylene, a straight chain polymer on their surface.

2.5. Cytotoxicity evaluation

The *in vitro* cytotoxicity study of Inu12-SLNs and Inu18-SLNs was conducted on Caco-2 cells. SLNs prepared with P188 and Tween-80 as the emulsifiers (P188-SLNs and Tween-SLNs) were used as the control groups. Meanwhile, cells without any treatment were used as a negative control group. The cell viability was assessed using cell counting kit-8 (CCK-8) assay to determine whether SLNs showed toxic effects at the concentration tested.

Figure 11 displays the cell viability of all formulations after incubation with the cells for 6 h. The viability of the cells treated with the four SLNs was all more than 85 %. Compared with P188-SLNs and Tween-SLNs, the cell viability of Inu12-SLNs and Inu18-SLNs had no significant difference ($P > 0.05$). This suggested that the toxic effects of Inu12 and Inu18 on cell viability showed no significant difference in comparison to P188 and Tween 80. The results preliminarily illustrated that Inu12 and Inu18, two CAM innovatively used as the emulsifier of SLNs in this study, were nontoxic at the concentration tested.

2.6. Conclusions

The comb-shaped amphiphilic alkylated inulin derivatives with different alkyl chains length (Inu12 and Inu18) were fabricated

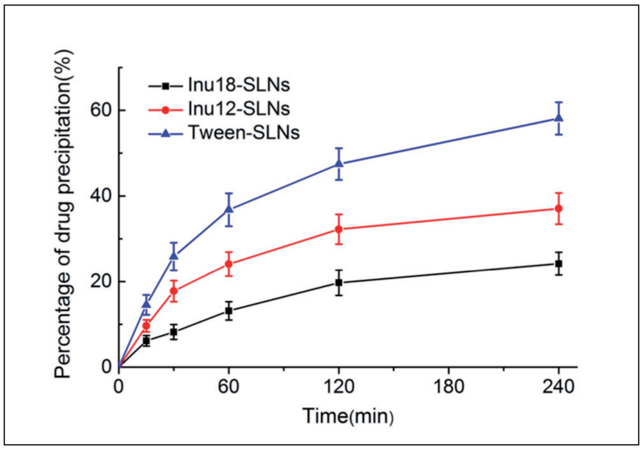

Fig. 9: Percentage of drug precipitation of CsA-loaded SLNs during lipolysis.

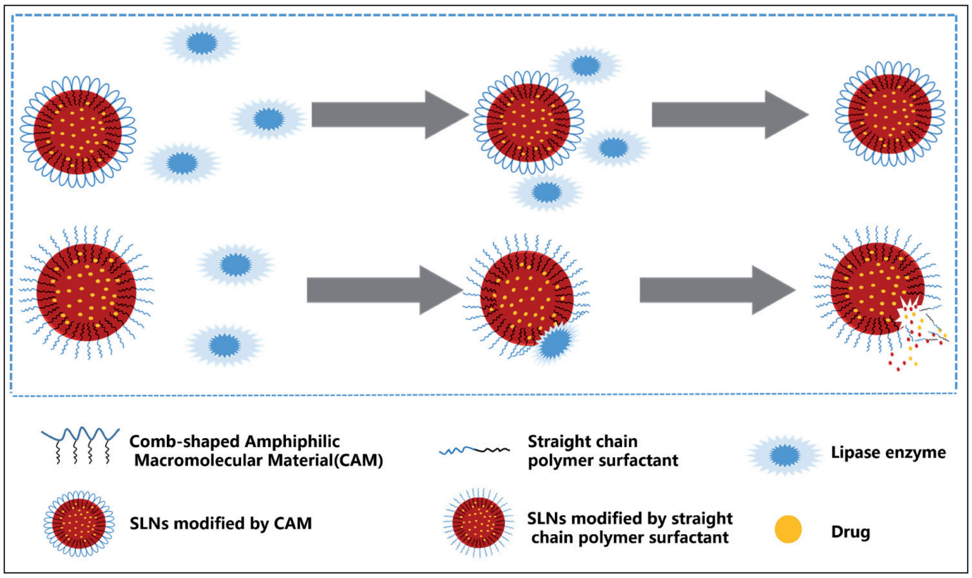

Fig. 10: Schematic possible mechanism of improved GIT stability of SLNs by CAM.

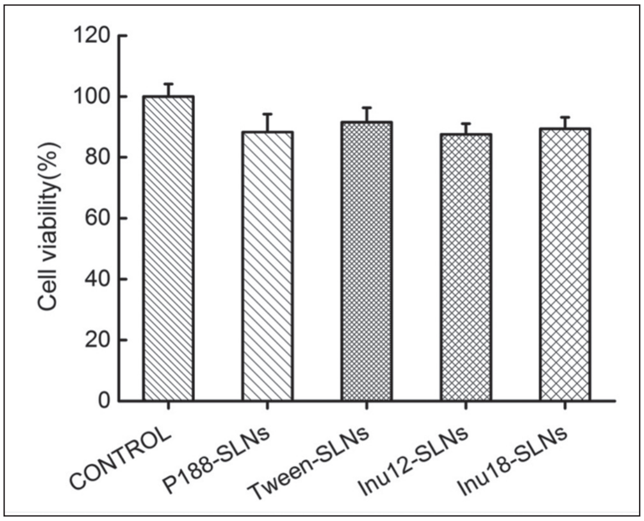

Fig. 11: CCK-8 assays of cell viability after incubation of SLNs with Caco-2 cells for 6h. Each date was expressed as the mean±SD (n=3).

for surface-modified SLNs to reduce the lipolysis and thereby improve the GIT stability of SLNs. As compared to the controlled P188/Tween-SLNs, the Inu12-SLNs and Inu18-SLNs showed a significantly reduced lipolysis, and Inu18-SLNs had the slowest lipolysis rate. Besides, the drug precipitation of CsA-loaded Inu18-SLNs and Inu12-SLNs were significantly lower than that of CsA-loaded Tween-SLNs, and Inu18-SLNs had the lowest drug precipitation during the lipid degradation. In general, it can be concluded that both inulin-derived CAM-modified SLNs, especially the Inu18-SLNs had the improved GIT stability to resist the lipid degradation by lipase enzyme. The possible reason for this was that hydrophilic backbone of Inu18 or Inu12, a kind of CAM, could form the sunflower-petal like loops on particle surface of SLNs (Fig. 2), resulting in a stronger steric hindrance effect against lipase enzyme compared with straight chain surfactant. The easy synthesis method of alkylated inulin derivatives by only one-step route, and this facile preparation of SLNs by melt-emulsification and ultrasonication method might make alkylated inulin-derived CAM-modified SLNs attractive in industrial-scale production. SLNs and the other nanoparticles modified with CAM (such as alkylated inulin derivations) instead of straight polymer (such as PEG) might also be used to achieve long circulation effect after intravenous injection, which need to be studied further.

3. Experimental

3.1. Materials

Inulin (Molecular Weight 5600 Da), molecular sieve (4 Å) and 1-methyl-2-pyrrolidinone (NMP) were supplied by Shanghai Aladdin Reagent Co., Ltd. (Shanghai, China). Octyl isocyanate, dodecyl isocyanate, and octadecyl isocyanate were purchased from Xi'a Reagent Co., Ltd. (Sichuan, China). Poloxamer 188 and Compritol® 888 ATO (glyceryl behenate) were gifted from Gattefossé (Saint-Priest, France). Tween-80 and acetone were obtained from Tianjin Damao Chemical Reagent Factory (Tianjin, China). Cyclosporine A (CsA, purity 99%) was supplied by Fujian Kerui Pharmaceutical Co., Ltd. (Fujian, China). Dialysis bags (Molecular Weight Cut-Off 8000-14000 and 3500) were from Solarbio Co., Ltd. (Beijing, China).

Lipase enzyme (from porcine pancreas), sodium taurodeoxycholate (NaTDC), Trizma® maleate were all purchased from Sigma-Aldrich (Saint-Louis, USA). 4-Bromobenzylboronic acid (4-BBBA) was bought from the company of Ark Pharm (Chicago, American). Bile salt (BS, 95%) and phospholipid (≥90%, from egg yolk) were obtained from Solarbio (beijing, china). All other chemicals were of analytical grade or HPLC grade. Cell counting Kit-8 was purchased from Boster Biological Technology Co., Ltd. (Hubei, China). Cell culture medium RPMI-1640, 0.25% trypsin-0.02% EDTA, and phosphate buffer solution (PBS) were all purchased from Solarbio Technology Co., Ltd. (Beijing, China). Fetal bovine serum (FBS) was obtained from TransGen Biotech Co., Ltd. (Beiing, China).

3.2. Synthesis of inulin derivatives

One-step synthesis route of alkyl inulin derivatives (Han et al. 2017; Kokubun et al. 2018; Stevens et al. 2001) was diagrammatized in Fig. 1. NMP (8.0 mL) and inulin (1.0 g) were predried by molecular sieves and a vacuum oven (70 °C, 24 h) before added into the volumetric flask, respectively. After inulin was completely dissolved in NMP at 80 °C, isocyanate (1 mL) was added into the solution. The reaction flash was filled with nitrogen and hermetically sealed by a sealing membrane to maintain a relatively independent environment. After the reaction was continued for 24 h at 80 °C, the reaction mixture was poured into 100 mL of refluxed acetone and stirred for 30 min. Then the mixture was transferred into a dialysis bag (MWCO: 3500 Da) and was dialyzed with distilled water for 48 h. The mixture in the dialysis bag was centrifuged (3000 rpm, 30 min) and filtered. The supernatant was freeze-dried and white flocculent alkyl inulin derivative was obtained.

Inulin derivative was characterized by FT-IR and ^1H NMR. The degree of substitution (DS) of isocyanate was determined using elemental analysis (EA). FT-IR spectra was recorded using Fourier-transform infrared spectrometer (8400, Shimadzu Corporation, Kyoto, Japan). After dissolved in D_2O, ^1H NMR spectrum of inulin derivatives was conducted using a nuclear magnetic resonance spectrometer (Bruker AVANCE 600 MHz, Zurich, Switzerland) at room temperature by scanning 32 times. Elemental analysis was performed using an Element Vario EL III analyzer (Vario EL III, Elementar, Germany). The degrees of alkylation substitution of inulin derivatives (DS) was estimated by the following equation:

$$C/N = 12\times(6+DS\times n)/(14\times DS) \quad (1)$$

where C/N was the content ratio of carbon to nitrogen, and n was the average number of carbon atom of alkyl group grafted.

3.3. *Preparation of SLNs*

SLNs were prepared by melt-emulsification and ultrasonication method (Walz et al. 2018) using Compritol® 888 ATO as lipid material, and CsA as model drug. Compritol 888 ATO (50 mg) and CsA (10 mg) were heated and maintained 10 °C above the melting point of lipid, so that all the lipid material as oil phase was melted. The aqueous phase was prepared by dissolving Inu8, Inu12, Inu18, Tween-80, or Poloxamer188 (50 mg) in distilled water (5 mL) and heated to the same temperature as that of oil phase.

Subsequently, the hot aqueous phase was poured into the oil phase with high-speed stirring (T18 basic ULTRA-TURRAX®, IKA-Werke, Staufen, Germany) at 11000 rpm for 3 min (Tween 80 or Poloxamer188 as emusifier) or 5 min (Inu8, Inu12 or Inu18 as emusifier). The coarse emulsion was ultrasonicated using a probe sonicator (SCIENTZ-II, Ningbo Scientz Biotecnology Co., Ltd., Zhejiang, China). CsA-loaded SLNs suspension was obtained by allowing the hot emulsion to cool down to room temperature. Empty SLNs were prepared following above procedure without the addition of CsA.

The SLNs prepared with Inu8, Inu12, Inu18, Tween 80, and Poloxamer188 as the emulsifier were nominated as Inu8-SLNs, Inu12-SLNs, Inu18-SLNs, Tween-SLNs, and P188-SLNs, respectively.

3.4. *Characterizations of SLNs*

3.4.1. *Morphology*

The morphology of SLNs was observed under a transmission electron microscope (TEM, JEM-2100, Japan Electronics Corporation, Tokyo, Japan). Samples were diluted 50-fold with distilled water, and 10 µL of the diluted SLNs samples were dropped on copper grids. After some of the solution volatilized, a drop of 2 % phosphotungstic acid solution was used for negative staining. Being dried for 12 h, the samples were observed under the transmission electron microscope.

3.4.2. *Particle size and zeta potential*

Particle size and zeta potential of SLNs were determined by Malvern Zetasizer (Nano ZS 90, Malvern Instruments Ltd., Worcestershire, UK).

3.4.3. *HPLC analysis of CsA*

Determination of CsA concentration for entrapment efficiency (EE), drug loading (DL), *in vitro* release studies was conducted by HPLC. HPLC determination was performed with an Agilent 1260 infinity liquid chromatography system (Agilent Technologies, California, USA). The system contained a 1260-Quaternary pump, a 1260-VWD UV/Vis detector, and a C18 column (Hypersil ODS, 4.6 mm × 200 mm, 5 µm; Elite, Liaoning, China). The mobile phase was a mixture of distilled water and acetonitrile (HPLC grade) at the ratio of 25:75 (*v/v*). Samples (20 µL) were injected into HPLC system with a flow rate of 1.0 mL/min at a column temperature of 65 °C and the UV detection was performed at 210 nm.

3.4.4. *Determination of encapsulation efficiency and drug loading*

CsA-loaded SLNs were diluted by 10% (w/v) ethanol and then ultra-centrifuged at 60,000 rpm for 30 min (Optima L-100K, Beckman Coulter Inc., Brea, CA, USA). The supernatant was determined for CsA concentration by HPLC. All experiments were done in triplicate to calculate encapsulation efficiency (EE) and drug loading (DL) by the following equations:

$$EE=(m_1-m_2)/m_1\times100\% \quad (2)$$

$$DL=(m_1-m_2)/m_0\times100\% \quad (3)$$

with m_1: total amount of CsA added m_2: free CsA m_0: weight of SLNs

3.5. *Drug release in vitro*

Phosphate buffer solution (PBS, pH=6.8) containing 0.10% (w/v) sodium dodecylsulfate (SDS) was used as *in vitro* release medium. After ultracentrifugation at 60,000 rpm for 30 min to remove free CsA, SLNs were resuspended in 10 mL of release medium, and 2 mL of equivalent SLNs suspension was loaded into a dialysis bag (MWCO: 15000) and dialyzed in a sealed brown bottle containing 50 mL release medium. The bottle was kept at 37±0.5 °C in a water bath Shaker (TH2-82, Xiaoyang, Jiangsu, China) shaking at 90 rpm. Samples (1 mL) were withdrawn from the release medium at predetermined intervals at 1, 2, 4, 6, 8, 10, 12, 24, 48, and 72 h respectively. Then the same volume of fresh medium was supplemented to the release medium at each time. The samples were filtered through a filter membrane (0.22 µm, Nylon 66, Millipore, Billerica, MA) and analyzed by HPLC.

3.6. *Gastrointestinal tract stability study*

3.6.1. *In vitro lipolysis tests on SLNs*

Lipase solution was prepared as the method described by Philip with some modification (Sassene et al. 2014). Sodium chloride (150 mM), calcium chloride (5 mM) and maleate (2 mM) were dissolvd in distilled water (Bolko et al. 2014; Thomas et al. 2012). The solution was adjusted to pH 6.5 by adding NaOH solution (0.2 M) and kept under 2-8 °C before the lipase was added. 5 mL of the solution was quickly added with 1 g of the lipase enzyme and then centrifuged at 6000 rpm (4 °C) for 15 min. The supernatant containing lipase with 600 USP/mL of enzyme activity was obtained.

Sodium chloride (150 mM), calcium chloride (5 mM), maleate (2 mM), NaTDC (3 mM), lecithin (0.75 mM) were dissolved in distilled water (Griffin et al. 2013; Heider et al. 2014; Dahan and Hoffman 2008). *In vitro* lipolysis medium was obtained by adjusting the solution to pH 6.5 (Dahan and Hoffman 2008). *In vitro* lipolysis of SLNs was conducted in the pH-stat apparatus (ZDJ-400, Automatic multi-function titrator, Beijing pioneer Weifeng technology development co, Ltd, china) equipped with a 100 mL thermostat glass reactor and a pH electrode. SLNs were completely dispersed in 30 mL of the *in vitro* lipolysis medium. The initial pH was manually adjusted to 6.5 with a little amount of NaOH or HCl solution and the lipolysis of SLNs was allowed to commence by the addition of 4 mL lipase solution pretreated as above. The medium in the reaction vessel was maintained a constant pH value of 6.5 by automatic addition of 0.2 M NaOH during the period of *in vitro* lipolysis. After 4 h of lipolysis, the lipolysis reaction was terminated by addition of 200 µL lipase inhibitor (4-BBBA, 1 M) (Heider et al. 2014; Dahan and Hoffman 2008). Back-titration to pH 9.0 was carried out by adding 1 M NaOH to the reaction vessel (Dahan and Hoffman 2008). Besides, the corresponding empty experiments without the addition of SLNs were performed for removing the degradation of impurities from crude pancreatic extract. The extents lipolysis during 4 h (E) was calculated by the following equation:

$$E=(N_1+N_2)/N\times100\% \quad (4)$$

where N_1 and N_2 were the consumptions of NaOH when SLNs were titrated at pH 6.5 and 9.0, respectively, N represented the theoretical maximum consumption of NaOH to neutralize the fatty acids from complete degradation of Compritol 888 ATO in SLNs.

3.6.2. *Determination of drug precipitation during lipolysis*

The lipolysis of CsA-loaded SLNs was conducted as the procedure described in Section 3.6.1. At predetermined time points of 15, 30, 60, 120, 240 min, 6 mL of samples was withdrawn and mixed with 30 µL lipase inhibitor to terminate the lipolysis reaction. After centrifugation at 60 000 rpm for 20 min, precipitation phase was obtained. Then precipitation phase was dispersed again with 6 mL ethanol aqueous solution (10%) and had the same centrifugation treatment again to separate free drug and SLNs. The supernatant was analyzed by HPLC to determine the drug precipitated from SLNs during lipolysis.

3.7. *Cell studies*

3.7.1. *Cell culture*

Human colon carcinoma Caco-2 cells were cultured in 25 cm^2 culture flasks with culture medium. The RPMI-1640 medium contained 10% fetal bovine serum, 1% non-essential amino acids, 1% l-glutamine, 100 mg/mL streptomycin and 100 IU/mL penicillin. The culture flasks were maintained in an incubator at 37 °C, 95% relative humidity, with 5% CO_2. The culture medium was exchanged everyday by fresh medium. When reaching 80% confluence, cells were harvested. Then they were detached from the culture flasks by trypsinization with 0.25% trypsin containing 0.05 mM ethylenediamine tetraacetic acid (EDTA), and diluted to a density of 1.0×10^5 cells/cm^2.

3.7.2. *Cytotoxicity*

The cytotoxic effect of SLNs was assessed using cell counting kit-8 (CCK-8) assay (Zhu et al. 2015). Caco-2 cells were seeded in a 96-well plate at 5×10^4 cells/cm^2 and incubated for 24 h with 200 µL culture medium under 37 °C and 5% CO_2. Then, cells were treated with 10 µL SLNs suspension for 6 h. Next, SLNs suspension in each well was replaced by 10 µL CCK-8 solution, and cells were further incubated for another 2 h. Finally, the absorbance of cell medium in each well was measured at 450 nm by a microplate reader (9602A, Beijing Perlong Medicare Co., Ltd. Beijing, China). The cells without any treatment were set as control. Every measurement was conducted in triplicate.

3.8. *Statistical analysis*

One-way analysis of variance (ANOVA) was used to determine significance between sample groups. A value of $P < 0.05$ was considered to be significant. All data were expressed as means±SD.

Acknowledgments: This work was supported by the National Natural Science Foundation of China (Grant No. 81560576 and 81760640) and the Innovation Special Fund of Nanchang University (Grant No. 240).

Conflict of interests: The authors have no conflicts of interest to declare.

References

Ban C, Jo M, Lim S, Choi Y J (2017) Control of the gastrointestinal digestion of solid lipid nanoparticles using PEGylated emulsifiers. Food Chem 239:442-452.

Bolko K, Zvonar A, Gašperlin M (2014) Simulating the digestion of lipid-based drug delivery systems (LBDDS): overview of *in vitro* lipolysis models. Acta Chim Slov 61: 1-10.

Christophersen P C, Zhang L, Müllertz A, Nielsen H.M, Yang M, Mu H (2014) Solid lipid particles for oral delivery of peptide and protein drugs II--the digestion of trilaurin protects desmopressin from proteolytic degradation. Pharm Res 31: 2420-2428.

Dahan A, Hoffman A (2008) Rationalizing the selection of oral lipid based drug delivery systems by an *in vitro*, dynamic lipolysis model for improved oral bioavailability of poorly water soluble drugs. J Control Release 129: 1-10.

De Jesus M B, Zuhorn I S (2015) Solid lipid nanoparticles as nucleic acid delivery system: Properties and molecular mechanisms. J Control Release 201: 1-13.

Exerowa D, Platikanov D (2009) Thin liquid films from aqueous solutions of non-ionic polymeric surfactants. Adv Colloid Interface Sci 147: 74-87.

Feeney OM, Williams HD, Pouton CW, Porter CJ (2014) ‘Stealth’ lipid-based formulations: poly(ethylene glycol)-mediated digestion inhibition improves oral bioavailability of a model poorly water soluble drug. J Control Release 192: 219-227.

Griffin BT, Kuentz M, Vertzoni M, Kostewicz ES, Fei Y, Faisal W, Stillhart C, O’Driscoll CM, Reppas C, Dressman JB (2013) Comparison of *in vitro* tests at various levels of complexity for the prediction of in vivo performance of lipid-based formulations: case studies with fenofibrate. Eur J Pharm Biopharm 86: 427-437.

Han L, Ratcliffe I, Williams P.A. (2017) Synthesis, characterisation and physicochemical properties of hydrophobically modified inulin using long-chain fatty acyl chlorides. Carbohydr Polym 178: 141-146.

Heider M, Hause G, Mäder K (2014) Does the commonly used pH-stat method with back titration really quantify the enzymatic digestibility of lipid drug delivery systems? A case study on solid lipid nanoparticles (SLN). Eur J Pharm Biopharm 109: 194-205.

Hoskins C, Thoo-Lin PK, Cheng WP (2012) A review on comb-shaped amphiphilic polymers for hydrophobic drug solubilization. Ther Deliv 3: 59-79.

Imran S, Gillis RB, Kok MS, Harding SE, Adams GG (2012) Application and use of inulin as a tool for therapeutic drug delivery. Biotechnol Genet Eng Rev 28: 33-45.

Jannin V, Dellera E, Chevrier S, Chavant Y, Voutsinas C, Bonferoni C, Demarne F (2014) *In vitro* lipolysis tests on lipid nanoparticles: comparison between lipase/co-lipase and pancreatic extract. Drug Dev Ind Pharm 24: 1-7.

Kokubun S, Ratcliffe I, Williams P A (2018) The interfacial, emulsification and encapsulation properties of hydrophobically modified inulin. Carbohydr Polym 194: 18-23.

Małgorzata G M, Michał M (2016) Solid lipid nanoparticles as attractive drug vehicles: Composition, properties and therapeutic strategies. Mater Sci Eng C Mater Biol Appl 68: 982-994.

Morros J, Levecke B, Infante M R (2010) Chemical hydrophobic modification of inulin in aqueous media: Synthesis of β-hydroxyalkyl ethers of inulin. Carbohydr Polym 81: 681-686.

Sassene P, Kleberg K, Williams H D (2014) Toward the establishment of standardized *in vitro* tests for lipid-based formulations, part 6: effects of varying pancreatin and calcium levels. AAPS J 16: 1344-1357.

Shidhaye SS, Vaidya R, Sutar S, Kadam VJ (2008) Solid lipid nanoparticles and nanostructured lipid carriers – innovative generations of solid lipid carriers. Curr Drug Deliv 5: 324-331.

Stevens CV, Meriggi A, Peristeropoulou M, Christov PP, Booten K, Levecke B, Vandamme A, Pittevils N, Tadros TF (2001) Polymeric surfactants based on inulin, a polysaccharide extracted from chicory. 1. synthesis and interfacial properties. Biomacromolecules 2: 1256-1259.

Tadros T (2009) Polymeric surfactants in disperse systems. Adv Colloid Interface Sci 147: 281-299.

Talele P, Sahu S, Mishra A K (2018) Physicochemical characterization of solid lipid nanoparticles comprised of glycerol monostearate and bile salts. Colloids Surf B Biointerfaces 172: 517-525.

Thomas N, Holm R, Rades T, Müllertz A (2012) Characterising lipid lipolysis and its implication in lipid-based formulation development. AAPS J 14: 860-871.

Thukral DK, Dumoga S, Mishra AK (2014) Solid lipid nanoparticles: promising therapeutic nanocarriers for drug delivery. Curr Drug Deliv 11: 771-791.

Torchilin VP (1998) Polymer-coated long-circulating microparticulate pharmaceuticals. J Microencapsul 15: 1-19.

Walz M, Hagemann D, Trentzsch M, Weber A, Henle T (2018) Degradation studies of modified inulin as potential encapsulation material for colon targeting and release of mesalamine. Carbohydr Polym 199: 102-108.

Wang T, Bae M, Lee J Y, Luo Y C (2018) Solid lipid-polymer hybrid nanoparticles prepared with natural biomaterials: A new platform for oral delivery of lipophilic bioactives. Food Hydrocoll 84: 581-592.

Warren DB, Bergström CA, Benameur H, Porter CJ, Pouton CW (2013) Evaluation of the structural determinants of polymeric precipitation inhibitors using solvent shift methods and principle component analysis. Mol Pharm 10: 2823-2848.

Warren DB, Benameur H, Porter CJ, Pouton CW (2010) Using polymeric precipitation inhibitors to improve the absorption of poorly water-soluble drugs: A mechanistic basis for utility. J Drug Target 18: 704-731.

Zhang X, Zhang YW, Zhang HY, Yang QY, Wang HY, Zhang GC (2015) Preparation and structural characterization of octenyl succinic anhydride modified inulin. Int J Biol Macromol 78: 79-86.

Zhu S, Chen S, Gao Y, Guo F, Li FY, Xie BG, Zhou JL, Zhong HJ (2015) Enhanced oral bioavailability of insulin using PLGA nanoparticles co-modified with cell-penetrating peptides and Engrailed secretion peptide (Sec). Drug Deliv 23: 1980-1991.